

Behavioral Study of Various Radial Basis Functions for Approximation and Interpolation Purposes

Martin Cervenka
 University of West Bohemia
 Pilsen, Czech Republic
 cervemar@kiv.zcu.cz¹

Vaclav Skala
 University of West Bohemia
 Pilsen, Czech Republic
 http://www.VaclavSkala.eu

Abstract— Both approximation and interpolation are techniques commonly used in many scientific areas. Many approaches are depending on input data type, result purpose etc. Input data can be formed in a mesh or not (meshless/meshfree data).

This contribution is oriented on meshless data approximation and interpolation using Radial Basis Functions (RBFs). Different RBFs behaves differently, but many of them have a shape parameter. This paper compares various RBFs concerning its shape parameters and provides some experimental results for each of the selected RBF.

Index Terms—RBF, radial basis function, interpolation, approximation, shape parameter, axis scaling

I. INTRODUCTION

There are many areas for approximation and interpolation in using RBF methods, despite the fact its higher computational cost. Biancolini [1], Menandro [2] and Fasshauer [3] used RBF methods in engineering practise. The RBF technique can be also used for image reconstruction [4], GIS systems [5], meteorology [6], partial differential equations [7], [8] etc.

There are two main groups of data representation i.e. mesh-based and meshfree/meshless. In the case of mesh-based data, a structure of the data is well-known apriori, in opposite to meshfree data, which are scattered in space. Meshfree data lack of connectivity information, so it is typically harder to approximate/interpolate.

Tessellation can be made to transform scattered data (mesh-free) to structured data (mesh). A common tessellation technique is Delaunay triangulation, however, its computational complexity is $O(n^{\lceil d/2 \rceil + 1})$ in d -dimensional space, i.e. for $d = 2$ is $O(n^2)$ and for $d = 3$ is $O(n^3)$ (more in Smolik [9]).

Dimension of the data is important, too. The higher the dimension is, the more complex and time-consuming algorithm is used. This is not completely true in the case of RBF approximation, which is nearly independent of problem dimensionality. Another advantage, which RBF technique brings, is that RBF approximation and interpolation is invariant to all rigid Euclidean transformations. It means that it is indifferent whether RBF is used and then transformation is made or the other way around.

The research was supported by the Czech Science Foundation (GACR) project No.GA 17-05534S and partially by SGS 2019-016 project.

¹ Corresponding author

The RBF method is relatively old (Hardy [10], 1971), but there are still many issues to deal with. Some of them are described in the following.

This contribution is focused to determine the behaviour of RBF approximation under certain conditions:

- when RBF shape parameter varies (see "Shape parameter selection"),
- how is approximation or interpolation affected by scaling the X (domain) axis of the original approximated function.

II. RADIAL BASIS FUNCTION

A radial basis function is a function, which value depends only on the distance from one single point, called centre. It means that distance is the only independent variable of the RBF, following notation will be used from now on:

$$\varphi(\|\mathbf{x} - \xi\|) \quad (1)$$

Where ξ is RBF φ centre coordinate point and \mathbf{u} is arbitrary independent point in the space. $\|\mathbf{x}\|$ denotes euclidean norm of vector \mathbf{x} . It means that the RBF is a single variable function returning a single variable as well.

There are two groups of RBF in general:

- *global* radial basis function is not limited and affects whole space
- *local* radial basis function, which has zero value from some radius and further

A. Global RBF

A typical global RBF function is Gaussian RBF, which is defined as:

$$\varphi(r) = e^{-\alpha r} \quad (2)$$

Plot of this function is a Gaussian bell curve, which has non-zero values on \mathbb{R} . It means that this function influences the whole space (will be explained later on).

Another well-known global RBF is thin-plate spline (TPS), which is defined in (3).

$$\varphi(r) = r^2 \log r = \frac{1}{2} r^2 \log r^2 \quad (3)$$

There are many various global RBF. In this paper, proposed RBF global function with variable exponent is discussed, too:

$$\varphi(r) = r^2 (r^\alpha - 1) \quad (4)$$

B. Local RBF

Local RBFs are then defined in (5). This kind of functions has been introduced by Wendland [11], more of them can be found in paper from Skala [12]. It is nothing more than multiplication of polynomial $P(r)$ with some power of cutted polynomial $1-r$ (+ sign denotes that all negative values are changed to zero), so its value will not be negative.

$$\varphi(r) = (1-r)_+^q P(r)$$

$$\varphi(r) = \begin{cases} (1-r)^q P(r) & 0 \leq r \leq 1 \\ 0 & r > 1 \end{cases} \quad (5)$$

From the group of local radial basis function, it is worth mentioning the simplest local RBF:

$$\varphi(r) = (1-r)_+ \quad (6)$$

If higher power and a reasonable polynomial is used, the resulting RBF can be defined as:

$$\varphi(r) = (1-r)_+^7 (16r^2 + 7r + 1) \quad (7)$$

In this paper, four RBFs defined above are used and plotted together in Fig.1.

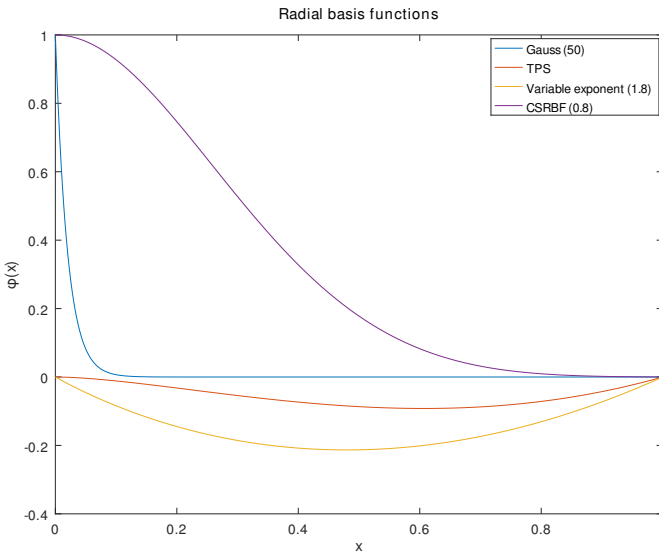


Fig. 1: Plot of the selected RBFs.

In the case of TPS and RBF with variable exponent, both functions "start" in 0 ($f(0) = 0$) and go directly through zero once more ($f(1) = 0$), then they rise to infinity ($\lim_{x \rightarrow +\infty} f(x) = +\infty$). The other two functions (Gaussian and CSRBF) "start" in 1 ($f(0) = 1$) and fall to zero ($\lim_{x \rightarrow +\infty} f(x) = 0$), CSRBF with given shape parameter λ (0.8) even satisfies $f(x) = 0, \forall x \geq 1.25$.

Using a weighted sum of infinitely many these elementary functions, it is possible to describe any function. In reality, however, there is a limit on how many RBF is used. In this case, the input function is not described precisely but is only approximated.

III. RBF APPROXIMATION

Function approximation using RBF is done using formula (8). In order to be able to solve this equation, all N RBF center points ξ_j has to be known apriori as well as eventual shape parameter(s) α_i of each RBF φ . Weights λ_j are unknowns and will be computed.

$$h(\mathbf{x}) = \sum_{j=1}^M \lambda_j \varphi(\|\mathbf{x} - \xi_j\|) = \sum_{j=1}^M \lambda_j \varphi(r_j) \quad (8)$$

Where N is number of points and M is number of reference points (centres). The introduced equation can be expressed in matrix form, which leads to system of linear equations:

$$\mathbf{Ax} = \mathbf{b}, \quad A_{ij} = \varphi_{ij}, \mathbf{b} = h_i, \mathbf{x} = \lambda_j, N > M, i = 1, \dots, N \quad (9)$$

Matrix \mathbf{A} is the rectangular matrix in general and the over-terminated system is obtained. There are several methods to solve the overdetermined system of equations. To minimize mean square error, the Ordinary Least Squares method (OLS) is used. Weights λ_j can be computed using OLS method by pseudoinverse as:

$$\lambda = (\mathbf{A}^T \mathbf{A})^{-1} \mathbf{A}^T \mathbf{h} \quad (10)$$

The solution of this equation leads to good approximation. However, Skala [13] shows that there may be some instability problems. Moreover, Majdisova [14] proved that in case of solving this equation via OLS additional polynomial conditions cannot be included.

IV. RBF INTERPOLATION

The RBF interpolation differs mathematically from approximation. In this case only distances between center points are considered. Equation for the RBF interpolation shown below:

$$h(\mathbf{x}_i) = \sum_{j=1}^N \lambda_j \varphi(\|\mathbf{x}_i - \mathbf{x}_j\|) = \sum_{j=1}^N \lambda_j \varphi(r_{ij}) \quad (11)$$

It is possible to rewrite this equation to matrix form the same way as in approximation (equation (9)). In approximation, resulting matrix is rectangular in general, whereas in this case the result \mathbf{A} is a square matrix of the linear equation system.

In opposite of approximation, the matrix \mathbf{A} can be further extended with polynomial conditions, now. The extended system is shown in formula (12).

$$\begin{bmatrix} \mathbf{A} & \mathbf{P} \\ \mathbf{P}^T & \mathbf{0} \end{bmatrix} \begin{bmatrix} \lambda \\ \mathbf{a} \end{bmatrix} = \begin{bmatrix} \mathbf{h} \\ \mathbf{0} \end{bmatrix} \quad (12)$$

The matrix \mathbf{P} represents polynomial additional conditions, λ is a vector of RBF weights, vector \mathbf{a} contains resulting polynomial coefficients, N is number of points and \mathbf{h} are given values at the given points, see Skala [15].

According to Jäger [16] and Skala [17] [18], in some cases it can be counterproductive to introduce polynomial conditions, especially for large scope of domain data.

V. RBF CENTRES PLACEMENT

The placement of RBF functions (setting their centre points) is another task to solve. A naïve method is to uniformly sample input function, but it does not take function properties into account. Despite this fact sometimes this approach is used, e.g. Singh [19]. Orr [20] in his paper proposes a regularization method, Wright [21] brings an improvement of this method near function boundaries. Majdisova et. al. [22] compare different techniques of RBF placement. In this paper, the geometrical properties of input signals are considered. RBFs are placed where input signals reach minima, maxima (1st order derivative is zero), inflexion points (2nd order derivative is zero) and to locations where 3rd order derivative is zero as well. This approach is inspired by [15], whereas in this paper there is a 1 $\frac{1}{2}$ D dimensional case (single parameter function) instead of 2 $\frac{1}{2}$ D (double parameter function). An example is shown in Fig.2, red crosses denote these points.

Function boundaries are often problematic, because there may not be any geometrically important points (minima, maxima, etc.). To solve this issue, artificial centres are added to the exact border. Even with this modification, the largest errors are still located near boundaries. This is solved by adding more points near boundaries. In 1 $\frac{1}{2}$ D case, four points should solve this issue (placed to 0%, 5%, 95% and 100% ratio of the domain space).

At this point, geometrically important points are covered, but it may happen that there will be a large "gap" between two consecutive centre points. One of the solution is to force minimal constant frequency, so large gaps will be filled with one or more another centre points.

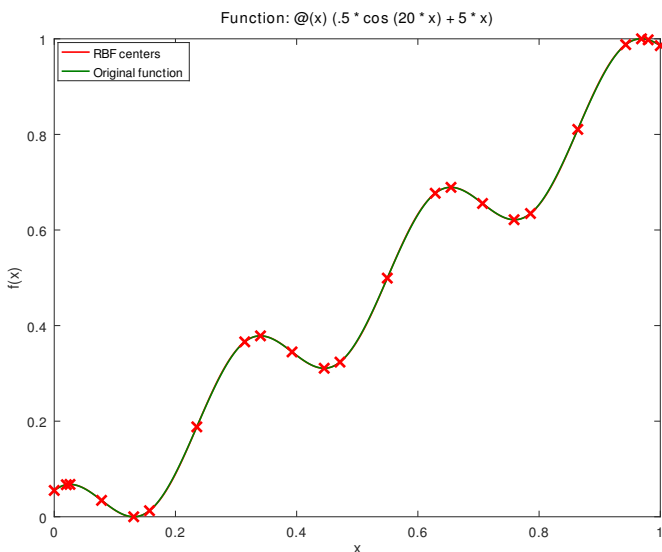


Fig. 2: Geometrically important points. The extension of this approach to the 2 $\frac{1}{2}$ D case was already explored by Vasta [23].

VI. SHAPE PARAMETER SELECTION

The selection of the shape parameter is a crucial part to do accurate interpolation or approximation. Shape parameter

can be selected for each RBF independently, which has an advantage of more precise results, on the other hand, all shape parameter values have to be stored then. A task of independent selection is an open question. Experiments from Skala, Karim and Zabran [24] showed, that there is probably no optimal global shape parameter. Suitable parameter selection is proposed by Wang and Liu [25], Afiatodust and Esmailbeigi [26] (using genetic algorithm) or Sarra and Sturgill [27] (random non-deterministic approach), however, none of them can find optimal shape parameter for each RBF. Optimal selection is due to this fact still an open question.

To simplify the problem, one single *global* shape parameter can be selected for all of RBFs, which results in less accurate approximation in general, but there is no need to store all values of shape parameters. In this case for each RBF one global shape parameter has been empirically selected in experiments described below.

VII. EXPERIMENTAL RESULTS

For testing purposes, we used 18 different functions (see Tab. I) taken from [15]. These functions, when approximated, discover various behaviour of chosen RBF approximation approach.

1	$\sin(15x^2) + 5x$
2	$0.5 \cos(20x) + 5x$
3	$50(0.4 \sin(15x^2) + 5x)$
4	$\sin(8\pi x)$
5	$\sin(6\pi x^2)$
6	$\sin(25x + 0.1)/(25x + 0.1)$
7	$2 \sin(2\pi x) + \sin(4\pi x)$
8	$2 \sin(2\pi x) + \sin(4\pi x) + \sin(8\pi x)$
9	$-2 \sin(2\pi x) + \cos(6\pi x)$
10	$2 \sin(2\pi x) + \cos(6\pi x)$
11	$-2 \sin(2\pi x) + \cos(6\pi x) - x$
12	$-2 \cos(2\pi x) - \cos(4\pi x)$
13	$\text{atan}((10x - 5)^3) + 0.5 \text{atan}((10x - 8)^3)$
14	$(4.48x - 1.88) \sin((4.88x - 1.88)^2) + 1$
15	$e^{10x-6} \sin((5x - 2)^2) + (3x - 1)^3$
16	$(1/9) \tanh(9x + 0.5)$
17	$\frac{6}{(1+16(x+0.5)^2) + \log(0.01*(x-.25)^2 + 10^{-5}) + 4}$
18	$\frac{6}{(1+16(x+0.5)^2) + \log(0.01*(x-.25)^2 + 10^{-10}) + 4}$

TABLE I: Tested artificial signals (taken from [15], extended).

For simplification of comparison, all 18 input signals have been tested for $x \in \langle 0, 1 \rangle$ and for simple comparison of errors all values in given domain have been scaled to $f(x) \in \langle 0, 1 \rangle$ as well. Mean square error and condition number of matrix \mathbf{A} (from equation (9)) are quantitative criteria for following tests.

A. Detecting geometrically significant points

Geometrically significant points are points with special properties. Special properties can be anything, in this case

special points are points which n -th derivative is zero, meaning:

$$f^{(n)}(x) = 0 \quad (13)$$

There are two groups of methods of how to detect significant points. One of them works in discrete space, the other in continuous space. To get these points in continuous space, either analytical solution of equation (13) is needed or numerical solution is required (gradient descent etc.).

In this paper, discrete space detection is selected. In this case, the function is sampled to N points (specifically 1000 points in this paper), which are denoted a_n . To get local extrema, differentiation is done, as follows:

$$a'_n = a_{n-1} - a_n \quad (14)$$

When consecutive elements a'_n and a'_{n+1} differs in sign, then local extrema is detected (difference go opposite way in two consecutive elements). If the differentiation is done twice, inflexion points are detected. It is possible then to continue with higher-order differentiation. In this paper it is done at most three times.

Short explanation: three-element signal $[3, 5, 4]$, which has obvious local extrema (maximum) of 5. After differentiation, $[-2, 1]$ vector is obtained. An only consecutive pair of elements differs in sign, meaning there were a local extrema.

This simplistic approach is sufficient for smooth functions, on noisy signal it would detect much more points than it should (smoothing is required).

B. Influence of the shape parameter

To test how much dependent the resulting approximation to shape parameter selection is, the range of the parameters is used. For every shape parameter, mean square error and condition number (of the matrix \mathbf{A} in equation (9)) are computed and showed in the following figures.

The first RBF tested is global Gaussian RBF. There are plotted results of mean square error depending on the selected shape parameter in Fig.3. It seems that the lower shape parameter α is selected, the lower average error is reached, but some functions do not respect this trend. It is risky to select lower shape parameter (e.g. $\alpha < 20$), but for some functions it gives the best result.

Condition number values of the matrix \mathbf{A} are presented in Fig.4. The higher value of shape parameter α is chosen, the better conditionality the problem has.

On the other hand, RBF $r^2(r^\alpha - 1)$ behaves the other way around. The higher shape parameter is selected, the lower error is possible to get, but it has worse conditionality at this point. Results are plotted in Fig.5 (mean square error) and Fig.6 (conditionality). There are some peaks (singularities) on this plot, which are caused by selecting the whole number as the shape parameter α .

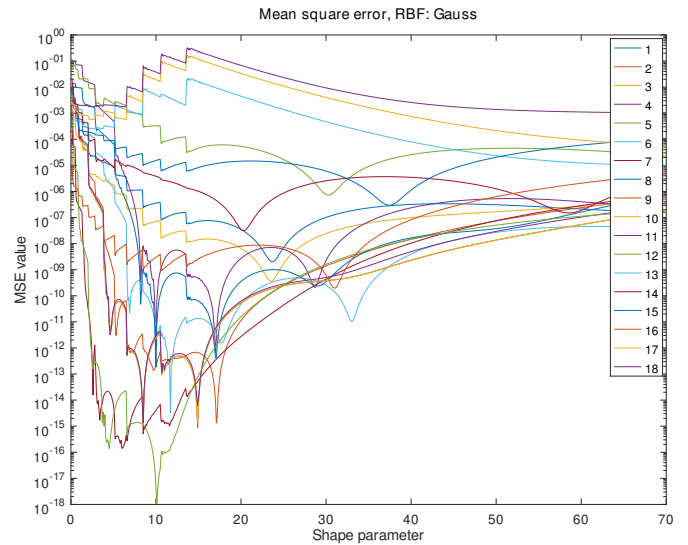


Fig. 3: Mean square error for Gaussian RBF. Note logarithmic scale on Y axis.

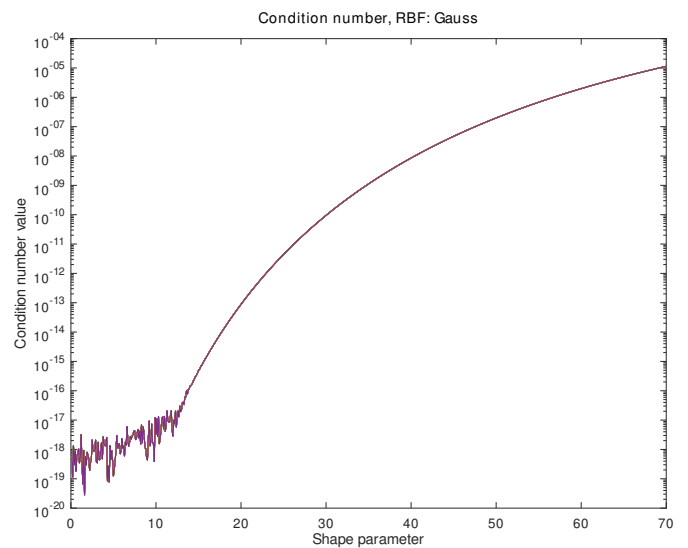


Fig. 4: Condition number values for Gaussian RBF. Note logarithmic scale on Y axis.

C. Influence of X-axis scaling

Idea is that scaling of the X-axis should influence resulting approximation error. This test stretches or squishes X-axis. Scaling X-axis is a similar operation to changing shape parameter, but these two operations are not linear in general. It should be noted that shape parameters are fixed during this test.

VIII. CONCLUSION

Different RBF functions have different properties and different behaviour in respect to its parameter(s), even using different signal which has to be approximated and does not have a significant impact. It seems there is a pattern between various

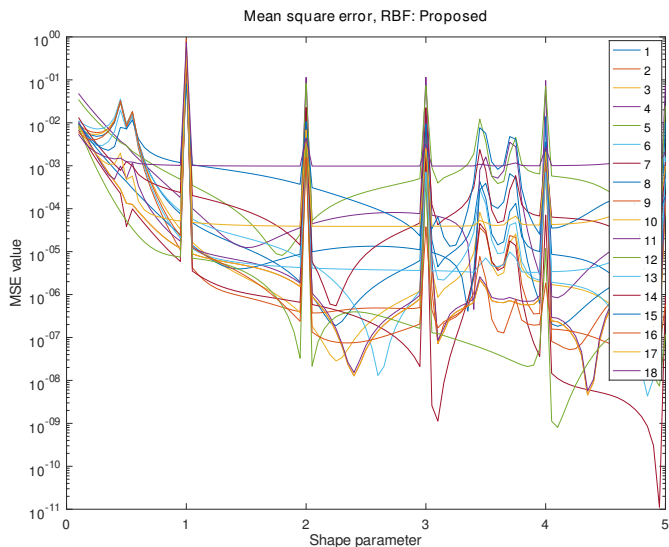


Fig. 5: Mean square error for proposed RBF. Note logarithmic scale on Y axis.

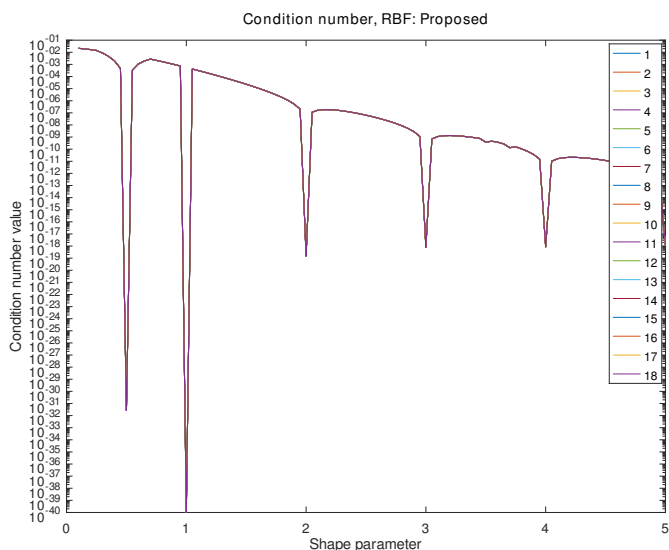


Fig. 6: Condition number values for proposed RBF. Note logarithmic scale on the Y-axis.

approximated signals as far as RBFs with same parameters are used and it is currently under investigation.

The tests with X-axis scaling show that the Gaussian RBF tends to have worse conditionality while scaling down, but it may reach lower approximation error. Second tested RBF seems to be independent to scaling (except one singularity) if approximation error is considered, conditionality is good without scaling, it is getting worse when scaling is applied.

Presented results show that there is a tradeoff between precision and conditionality in general. Selected shape parameter is due to this fact dependent on the predefined goal, which should be achieved. If the low error is requested, scaling down the X-axis may help. If the conditionality has to be high, scale-up may help in that case. This study may help to

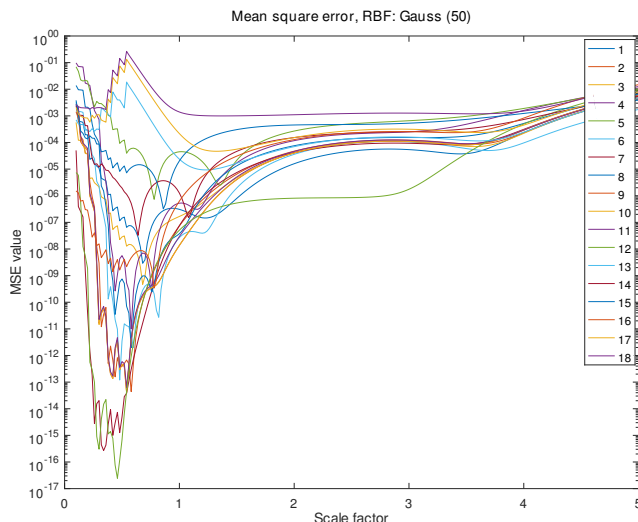


Fig. 7: Mean square error for Gaussian RBF. Note logarithmic scale on Y axis.

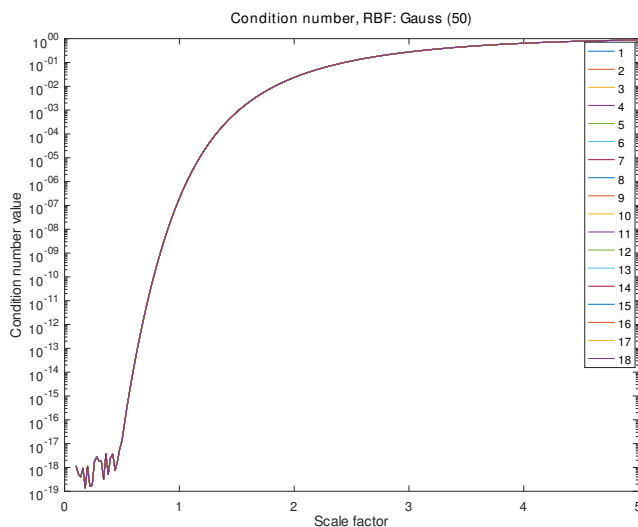


Fig. 8: Condition number values for Gaussian RBF. Note logarithmic scale on Y-axis.

select appropriate scaling factor as well as shape parameter, according to the approximation goal.

ACKNOWLEDGMENT

The authors would like to thank their colleagues and students at the University of West Bohemia for their suggestions and discussion. Authors would like to thank also to anonymous reviewers for their valuable comments, provided hints, and suggestions.

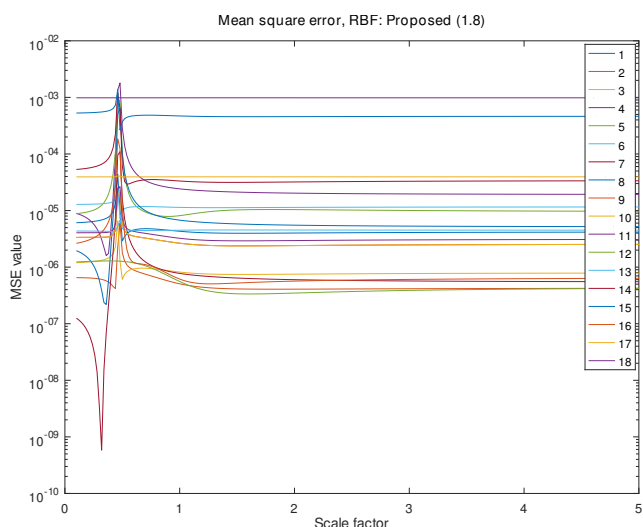


Fig. 9: Mean square error for proposed RBF. Note logarithmic scale on Y-axis.

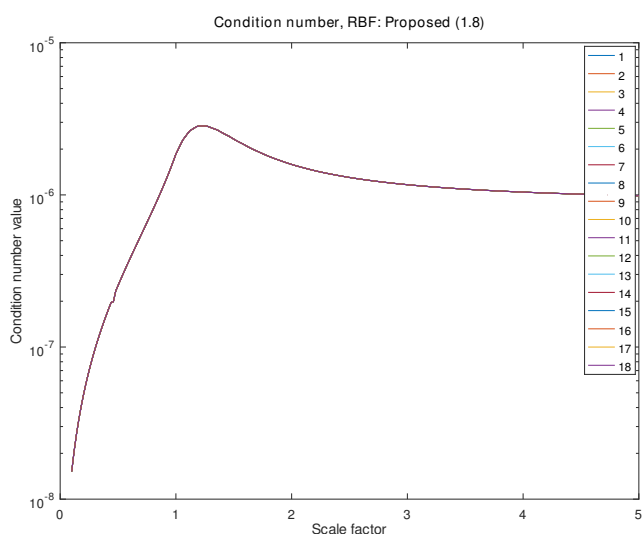


Fig. 10: Condition number values for proposed RBF. Note logarithmic scale on Y-axis.

REFERENCES

[1] M. E. Biancolini, *Fast Radial Basis Functions for Engineering Applications*, 1st ed. Springer International Publishing, 2017.

[2] F. Menandro, "Two new classes of compactly supported radial basis functions for approximation of discrete and continuous data," *Engineering Reports*, vol. 2019;1:e12028, pp. 1–30, 2019.

[3] G. Fasshauer, *Meshfree Approximation Methods with Matlab*, 1st ed. World Scientific, 2007.

[4] K. Uhlir and V. Skala, "Reconstruction of damaged images using radial basis functions," *13th European Signal Processing Conference, EUSIPCO 2005*, 01 2005.

[5] R. Pan and V. Skala, "Surface reconstruction with higher-order smoothness," *The Visual Computer*, vol. 28, no. 2, pp. 155–162, Feb 2012. [Online]. Available: <https://doi.org/10.1007/s00371-011-0604-9>

[6] D. Pepper, C. Rasmussen, and D. Fyda, "A meshless method using global radial basis functions for creating 3-d wind fields from sparse meteorological data," *Computer Assisted Methods in Engineering and Science*, vol. 21, no. 3/4, pp. 233–243, 2017. [Online]. Available: <https://cames.ippt.pan.pl/index.php/cames/article/view/42>

[7] E. Larsson and B. Fornberg, "A numerical study of some radial basis function based solution methods for elliptic PDEs," *Computers & Mathematics with Applications*, vol. 46, no. 5, pp. 891 – 902, 2003. [Online]. Available: <http://www.sciencedirect.com/science/article/pii/S0898122103901519>

[8] Y.-C. Hon, B. Šarler, and D. fang Yun, "Local radial basis function collocation method for solving thermo-driven fluid-flow problems with free surface," *Engineering Analysis with Boundary Elements*, vol. 57, pp. 2 – 8, 2015, rBF Collocation Methods. [Online]. Available: <http://www.sciencedirect.com/science/article/pii/S0955799714002793>

[9] M. Smolik and V. Skala, "Fast parallel triangulation algorithm of large data sets in e2 and e3 for in core and out core memory processing," vol. 8580, 07 2014.

[10] R. L. Hardy, "Multiquadric equations of topography and other irregular surfaces," *Journal of Geophysical Research (1896-1977)*, vol. 76, no. 8, pp. 1905–1915, 1971. [Online]. Available: <https://agupubs.onlinelibrary.wiley.com/doi/abs/10.1029/JB076i008p01905>

[11] H. Wendland, "Computational aspects of radial basis function approximation," in *Topics in Multivariate Approximation and Interpolation*, ser. Studies in Computational Mathematics, K. Jetter, M. D. Buhmann, W. Haussmann, R. Schaback, and J. Stöckler, Eds. Elsevier, 2006, vol. 12, pp. 231 – 256. [Online]. Available: <http://www.sciencedirect.com/science/article/pii/S1570579X06800108>

[12] V. Skala, "RBF Interpolation with CSRBF of Large Data Sets," *Procedia Computer Science*, vol. 108, pp. 2433 – 2437, 2017, International Conference on Computational Science, ICCS 2017, 12-14 June 2017, Zurich, Switzerland. [Online]. Available: <http://www.sciencedirect.com/science/article/pii/S187705091730621X>

[13] —, "Least square method robustness of computations: What is not usually considered and taught," in *2017 Federated Conference on Computer Science and Information Systems*, 09 2017, pp. 537–541.

[14] Z. Majdisova and V. Skala, "A new radial basis function approximation with reproduction," *CGVCVIP 2016*, 04 2018.

[15] V. Skala and M. Cervenka, "Novel RBF Approximation Method Based on Geometrical Properties for Signal Processing with a New RBF Function: Experimental Comparison," *Informatics 2019*, 2019.

[16] J. Jäger, "Advances in radial and spherical basis function interpolation," Ph.D. dissertation, Justus-Liebig-Universität, Otto-Behaghel-Str. 8, 35394 Gießen, 2018.

[17] V. Skala, "RBF interpolation and approximation of large span data sets," in *MCSI 2017 – Corfu*. IEEE, 2018, pp. 212–218.

[18] —, "RBF interpolation with CSRBF of large data sets," in *ICCS 2017, Procedia Computer Science*, vol. 108. Elsevier, 2017, pp. 2433–2437.

[19] B. Singh and D. Toshniwal, "MOWM: Multiple Overlapping Window Method for RBF based missing value prediction on big data," *Expert Systems with Applications*, vol. 122, pp. 303 – 318, 2019. [Online]. Available: <http://www.sciencedirect.com/science/article/pii/S0957417418308340>

[20] M. J. L. Orr, "Regularization in the selection of radial basis function centers," *Neural Computation*, vol. 7, no. 3, pp. 606–623, 1995. [Online]. Available: <https://doi.org/10.1162/neco.1995.7.3.606>

[21] G. B. Wright, "Radial basis function interpolation: Numerical and analytical developments," Ph.D. dissertation, University of Colorado at Boulder, Boulder, CO, USA, 2003, aAI3087597.

[22] Z. Majdisova and V. Skala, "Radial basis function approximations: comparison and applications," *Applied Mathematical Modelling*, vol. 51, pp. 728 – 743, 2017. [Online]. Available: <http://www.sciencedirect.com/science/article/pii/S0307904X17304717>

[23] J. Vasta, V. Skala, M. Smolik, and M. Cervenka, "Modified Radial Basis Functions Approximation Respecting Data Local Features," *Informatics 2019 (IEEE proceedings, in print)*, 2019.

[24] V. Skala, S. Karim, and M. Zabran, "Radial Basis Function Approximation Optimal Shape Parameters Estimation: Preliminary Experimental Results," in *(submitted for publication)*. AIP Press, 2019.

[25] J. Wang and G. Liu, "On the optimal shape parameters of radial basis functions used for 2-d meshless methods," *Computer methods in applied mechanics and engineering*, vol. 191, pp. 2611–2630, 2002.

[26] F. Afiatdoust and M. Esmaeilbeigi, "Optimal variable shape parameters using genetic algorithm for radial basis function approximation," *Ain Shams Engineering Journal*, vol. 6, pp. 639–647, 2015.

[27] S. A. Sarra and D. Sturgill, "A random variable shape parameter strategy for radial basis function approximation methods," *Engineering Analysis with Boundary Elements*, vol. 33, pp. 1239–1245, 2009.